

Original Research

Spatial Heterogeneity of Driving Forces in Response to Carbon Emissions from Land Use at County-Level in Beijing-Tianjin-Hebei Region

Chao Tian, Linlin Cheng*, Tingting Yin

College of Geoscience and Surveying Engineering, China University of Mining and Technology (Beijing),
Beijing 100083, China

Received: 18 July 2022

Accepted: 10 September 2022

Abstract

Carbon emissions from land use (LUCE) is an increasingly serious problem in China, and the direction of carbon reduction in urban agglomerations is still unclear. This study aimed to identify the key factors that influence county-level LUCE and their response to LUCE in Beijing-Tianjin-Hebei (BTH) region. Based on multi-source data, our study calculated county-level LUCE and its spatiotemporal variations in BTH from 1992 to 2018. Random forest (RF) and geographically weighted regression (GWR) models were applied to discuss influential factors' impact and spatial response on LUCE by quantifying relative importance and spatial heterogeneity. The results show that county-level LUCE in BTH increased by 1300.04×10^4 t, with an average annual growth rate of 46.11% during 1992-2018, and exhibited prominent spatial autocorrelation, with higher-value counties mostly in the core areas and lower-value counties in the suburbs within BTH. The RF estimates were better than the multiple linear regression (MLR) estimates with an improvement in R^2 from 0.56 to 0.98. Population, urbanization, energy intensity, industry proportion, road network density and technical progress had effective explanatory power for county-level LUCE. In addition, GWR estimation shows that the main influencing factors demonstrated significant spatial heterogeneity, and the impacts of population, urbanization, economic, energy structure and road factors in the central core counties were significantly higher than in the northwestern and southern regions. Industrial structure and technology have the greatest impact in the southern and northeast counties. This study explores different causes of LUCE in different counties of urban agglomerations and the continuation of low-carbon control measures in BTH is required.

Keywords: spatial heterogeneity, carbon emissions from land use, county-level, influential factors, random forest model, geographically weighted regression

Introduction

Global warming caused by carbon emissions poses a threat to ecosystem change and socio-economic development and has become a hot topic in the field of ecological environment [1-2]. As one of the key drivers of regional carbon emissions, land use change has an important impact on the human surface ecosystem, contributing to the Earth's carbon cycle processes [3]. Additionally, land use change increases atmospheric carbon emissions, which are second only to human burning of fossil fuels in terms of their impact on atmospheric concentrations [4]. Since 2008, China's carbon emissions have reached 83.25×10^8 t, making it the world's largest carbon emitter, and its carbon emissions from land use change are 32.37×10^8 t accounting for about 1/2 of the total carbon emissions [5]. China has proposed to reach the carbon peak before 2030 and achieve carbon neutralization before 2060. Based on the target of 'double carbon' goals, how to develop low-carbon economy and achieve social sustainable development has become an important issue in China [6]. As an important part of Chinese economy, counties make important contributions to energy consumption [7-8], and the issue of land use carbon emissions (LUCE) at the county level still needs further attention. To achieve the 'double carbon' goals as soon as possible, the Chinese government needs accurate LUCE data, especially for county areas, to take carbon emission reduction measures for different regions.

Previous studies have extensively investigated LUCE, with particular attention to the following aspects: (1) calculation methods of LUCE and (2) spatial and temporal evolution characteristics and (3) analysis of influencing factors and driving mechanisms of LUCE. In the first part, many studies have been based on plant carbon pools in terrestrial ecosystem ecological [9], socio-economic data [6], and compensation coefficients [10] to estimate LUCE. Although many achievements have been made in LUCE studies at the provincial and municipal levels [5, 11], the formulation of urban carbon emissions strategies requires the estimation of carbon emissions at more detailed scales, such as the county scale. Yu [12] based on GDP data, selecting 18912 counties in China and analyzing county-level spatial patterns and key influencing factors of LUCE intensity. Zhi et al [13] adopted a top-to-bottom method to systematically analyze spatiotemporal variations and driving factors of LUCE in 22 counties in North China. Zhang et al [14] took 75 counties in Shanxi as examples, analyzed energy consumption from land use data, and explored carbon emission risks and influencing factors of each county. However, county-level carbon emission data in the urban statistical yearbooks are limited to a few cities, and therefore, references for energy consumption estimation at county-level LUCE are relatively limited. This increases the difficulty of exploring LUCE below the city level. Additionally, the variability of statistics

quality at different scales leads to calculation errors, making it difficult to formulate reasonable, targeted and efficient carbon reduction policies. In recent years, the development and improvement of remote sensing have led to the widespread use of nighttime light (NTL) in CO₂ emissions [15-16]. NTL is a useful method to directly reflect the intensity of anthropogenic activities, and has the advantage of free access, long time series, and large coverage [11]. Many studies have utilized NTL data to explore the issues such as urban expansion, economic development and energy consumption estimation [5, 15, 17].

In terms of the second aspect, some researchers used Moran's *I* index [4], elliptic standard deviation [18], Gini coefficient [19] and Theil index [5] to evaluate spatial-temporal variation of LUCE. Regarding to the drivers affecting LUCE, land use carbon emissions are closely related to human activities, and thus socioeconomic factors have a significant effect on LUCE [20-21]. GDP and population density are considered to be the greatest impact on LUCE [22-23], and areas with higher GDP and population density are more likely to produce carbon emissions. Local fiscal expenditure indirectly impacts LUCE at different stages of urbanization development [24]. The industrial structure is associated with the dynamic changes of LUCE [13]. On the one hand, excessive industrial agglomeration can lead to an increase in carbon emission intensity, while industrial agglomeration can bring about a scale effect of carbon emission reduction. Studies also suggest that there is an inverted "U" relationship between urbanization and LUCE [25]. Energy structure is a key indicator of regional energy efficiency and economic structure, and changes in energy consumption will directly affect the changes in LUCE [26]. Road network density also plays an important role in regional LUCE [27]. Technological advances facilitate the reduction of LUCE, such as alternative clean energy technologies and new energy technologies [2]. In addition, national planning and policies, such as land use policies and urban planning can greatly affect LUCE [23].

Methodologically, previous scholars used LMDI decomposition model [28], STIRPAT model [29], grey correlation degree [30] and environmental Kuznets curve [31] to explore the association between driving factors and LUCE, as well as to study the driving mechanisms of LUCE within regions. However, such studies usually use linear regression, in some cases when explaining the non-linear relationships between variables and their relative importance, these models are not suitable for analysis. Random forest (RF) models may address these issues. The advantage of this approach is that it is a no-multicollinearity machine-learning technique with high efficiency, strong interference resistance and generalization ability, which can explain the complexity of the relative importance of several influential factors [32-33]. Moreover, China consists of different cities with different geographical locations and economic development levels, such that the carbon emissions

and reduction strategies of regions vary among regions [6]. However, the exploration of the relationship between driving factors and LUCE takes less consideration of the effects of spatial non-stationarity and differences at county-level. The spatial models, such as geographically weighted regression (GWR) model, can better deal with spatial non-stationarity caused by different factors and are widely used to understand the spatial heterogeneity of different drivers [34-35]. In our study, RF and GWR models were used to reveal the response of driving factors to LUCE.

Rapid urbanization leads to changes in land use/cover, which in turn leads to changes in carbon sources and carbon sinks for different land types [3]. As one of the urban agglomerations with the largest economies in China, the Beijing-Tianjin-Hebei (BTH) region possesses the fastest economic development and the highest urbanization level in Eastern China. With the acceleration of regional economic integration, the region's land spatial patterns and landscape structure are gradually changing. This study aimed to explore spatial-temporal changes of LUCE at the county scale, as well as the key influencing factors of county LUCE, so as to reveal its spatial response process in BTH. For this purpose, here we calculated the LUCE of 196 counties in 13 cities and explored their spatial-temporal distribution patterns in the BTH by using the corrected nighttime light datasets, land use data and energy consumption statistics from 1992-2018. We further introduced RF to calculate the relative importance of anthropogenic factors on LUCE in the BTH region, and then used GWR model to generate spatial coefficient distribution of LUCE in the research area.

Material and Methods

Study Area

The BTH (113°04'E-119°53'E, 36°01'N-42°37'N) is approximately 216600 km², including Beijing, Tianjin and Hebei Province. The area is of temperate monsoon climate, and with a northwest to southeast sloping topography. By the end of 2016, the BTH consists of 13 cities and 196 counties. According to the Outline of Coordinated Development of the Beijing-Tianjin-Hebei Region promulgated by the Chinese government in 2015, BTH should not only become a highly integrated urban agglomeration in the world, but also explore a new path for global product development, resource sharing and land optimization [36]. The coordinated development strategy of BTH plays an important role in the sustainable development of regional socio-economics and complements each other with distinct advantages.

They are different systems, cultures, economies, as well as regional imbalances within the BTH [37]. In 2018, the resident population and GDP of BTH were 113 million and 75610 billion RMB, respectively.

The urbanization rate reached 75.36 %, with 86.50% in Beijing, 83.15% in Tianjin, and 56.43% in Hebei province, respectively. With rapid urbanization and intense human activities, the land use patterns of the research area have changed (Fig. 1).

Data Sources and Processing

The data used in the study included land use data, Operational Line Scan System (DMSP-OLS) and Suomi National Polar-orbiting Partnership-Visible Infrared Imaging Radiometer Suite (NPP-VIIRS) nighttime light composites, energy consumption statistics, and relevant county-level socio-economic data. All data were resampled at a spatial resolution of 1km×1km and projected into Lambert Azimuthal Equal Area Projection.

Land Use Data

Land use data of Landsat TM and ETM images for 1992, 2000, 2010 and 2018 were provided by the Geospatial Data Cloud Platform (<http://www.gscloud.cn/>) with a spatial resolution of 30 m×30 m. The data were atmospherically corrected in ENVI and geometrically corrected in GPS, respectively, with an accuracy of no less than 85%. In this study, the land types in BTH were classified into six categories: cropland, forestland, grassland, wetland, water bodies, construction land and unused land.

Nighttime Light Data

The DMSP/OLS and NPP-VIIRS nighttime light data were obtained from the National Oceanic and Atmospheric Administration (NOAA) of National Geophysical Data Center (NGDC) (<https://www.ngdc.noaa.gov/>). DMSP-OLS data were available at a spatial resolution of 900m×900m and included F10, F12, F14, F15, F16, and F18 satellite sensors from 1992-2013. The NPP-VIIRS nighttime light data were selected for the mean radiometric cloud-free products from 2012 to 2018. We obtained the DMSP/OLS nighttime light data for China by image reprojection, mutual correction, intra-year correction, and time series correction [16-17], and NPP-VIIRS was calculated on the basis of removing low and high value noise from the images, which in turn cropped the two datasets according to the BTH boundary. Furthermore, we selected a univariate quadratic polynomial regression model to integrate these two nighttime light datasets, and the NPP-VIIRS data from the established regression model were utilized to correct the DMSP-OLS data continuously, and finally obtained the nighttime light datasets from 1992-2018.

Socio-Economic Data

On the basis of data availability and literature review in the Introduction section, the factors of per

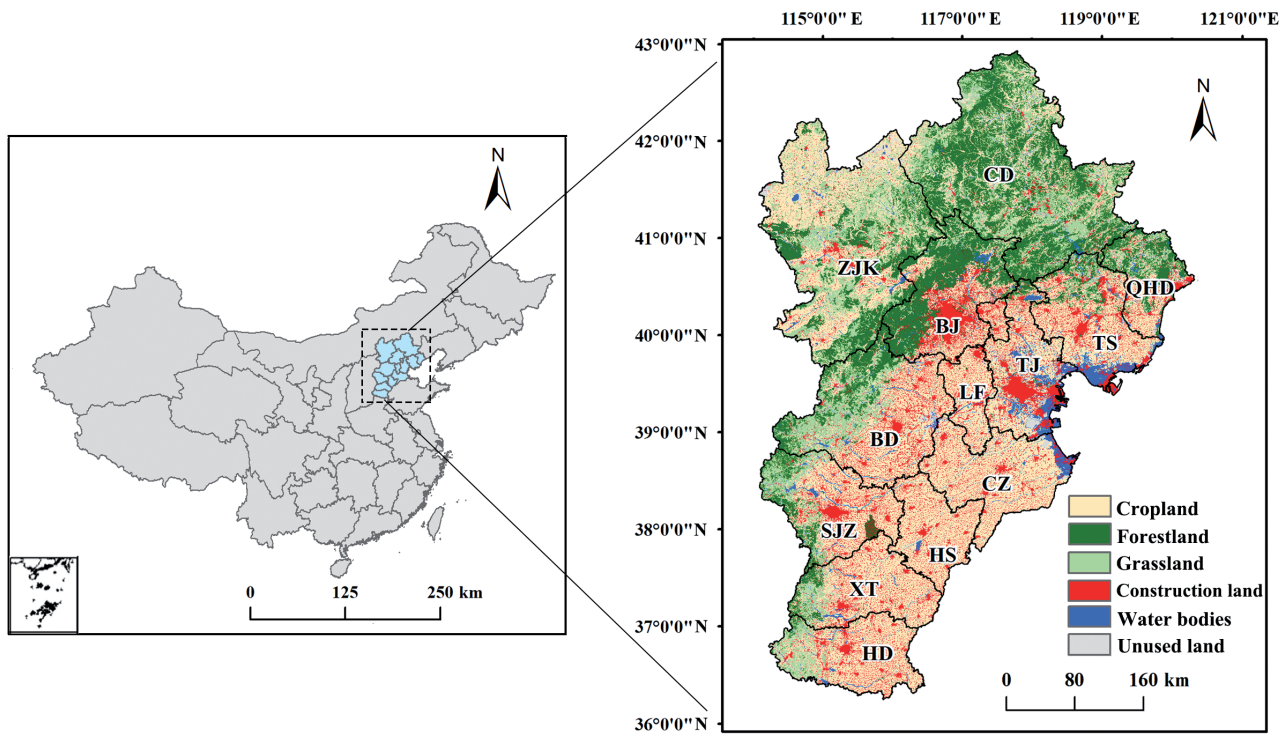


Fig. 1. Location of the study area The BTH includes 13 cities: Beijing (BJ), Tianjin (TJ), Shijiazhuang (SJZ), Tangshan (TS), Qinhuangdao (QHD), Handan (HD), Xingtai (XT), Baoding (BD), Zhangjiakou (ZJK), Chengde (CD), Cangzhou (CZ), Langfang (LF) and Hengshui (HS).

capita GDP (CGDP), local fiscal expenditure (LFE), primary industry proportion (PI), secondary industry proportion (SI), tertiary industry proportion (TI), population density (PD), urbanization rate (UR), energy structure (ES), road network density (RND), per capita land area (CLA), technological progress (TP), and land use policy (LUP) were chosen as influential factors. Socio-economic data were obtained from the statistical yearbook of each city, as well as China county statistical yearbooks. Road data were obtained from OpenStreetMap (OSM) (<https://www.openstreetmap.org/#map=4/36.96/104.17>), and RND was further calculated by ArcGIS. CLA was obtained from land use data. In this study, we used energy consumption per unit of GDP and the number of green patents of each county to represent energy structure and technological progress, respectively. Because policy factors are difficult to obtain and quantify, we selected the area of afforestation and grassland in counties that have a strong impact on LUCE.

Carbon Emissions Calculation Method

The processing steps of county-level LUCE were shown in Fig. 2. Specifically, we used carbon sink coefficients to calculate county-level carbon absorption, and the county-level carbon emissions were calculated based on the linear analysis between corrected nighttime light data and carbon emission statistics.

Estimation of Carbon Absorption from Land Use

The calculation formula of carbon absorption based on United Nations proposed by Intergovernmental Panel on Climate Change (IPCC) [38] list is as follows:

$$E_x = \sum A_i = \sum S_i \times T_i \quad (1)$$

Where E_x represents the direct carbon emissions (10^4t); A_i represents the carbon emissions of land use type i (Table 1); S_i represents the area of five land use types in BTH (hm^2); T_i represents the carbon emission coefficient of the land use type i ($t/(hm^2 \cdot a)$).

Estimation of LUCE Based on DMSP-OLS and NPP-VIIRS Nighttime Composites

Referring to the calculation method of *Guidelines for National Greenhouse Gas Inventory* of the IPCC, the formula of energy consumption of carbon emissions is as follows:

$$C = \sum_{i=1}^9 C_i = \sum_{i=1}^9 E_i \delta_i \quad (2)$$

Where C refers to carbon emission; E_i refers to the main consumption of energy sources i ; δ_i refers to the carbon emission coefficients of energy sources I , the coefficients were shown in Appendix Table 1.

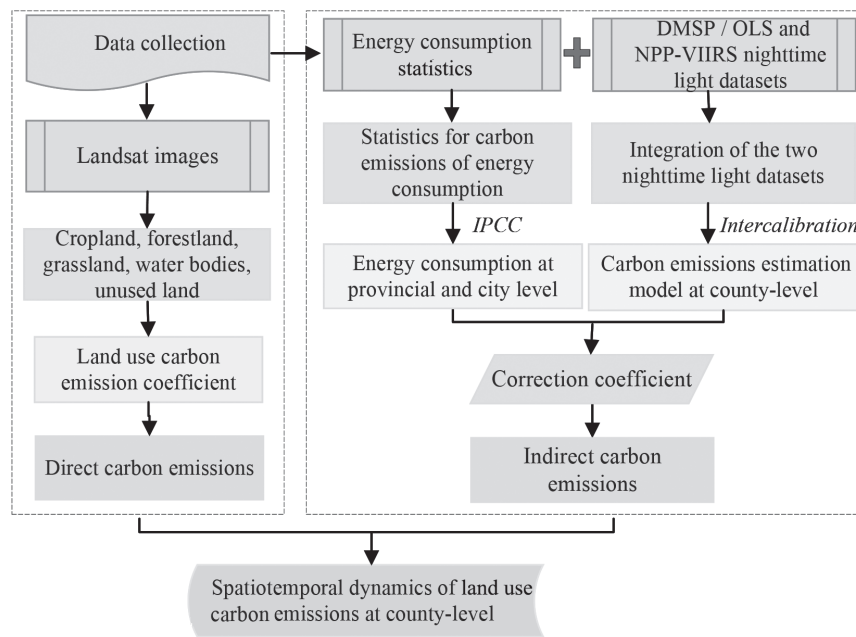


Fig. 2. Flowchart of land use carbon emissions processing.

We assumed a linear correlation between DN values and carbon emissions [37]. The equation can be expressed as follows:

$$E_i = aDN_i + b \tag{3}$$

Where E_i represents the estimation of carbon emission of county i ; DN_i represents the nighttime light value of county i ; a and b are regression parameters.

As shown in Table 2, the R^2 of the estimation models was all greater than 0.7, indicating that the results performed well. The regression coefficients of BTH also suggested a significant positive correlation between nighttime light datasets and carbon emissions, which is consistent with the original hypothesis, and meets the research requirements.

Spatial Autocorrelation Analysis

Spatial autocorrelation refers to the interdependence of spatial variables (LUCE) in a region [14]. In this

study, the global Moran's I and local Moran's I were used to explore the spatial aggregation characteristics of the county LUCE in BTH at global and local levels, and these formulas were calculated as follows:

$$I = \frac{\left[n \sum_{i=1}^n (x_i - \bar{x}) \sum_{j=1}^n w_{ij} (x_j - \bar{x}) \right]}{\left[\sum_{i=1}^n (x_i - \bar{x})^2 \sum_{i=1}^n \sum_{j=1}^n w_{ij} \right]} \tag{4}$$

$$G_i = \frac{\sum_{j=1}^n w_{ij} x_j}{\sum_{i=1}^n x_i} \tag{5}$$

Where n represents the number of counties in BTH; x_i and x_j represents LUCE of county i and j , respectively; \bar{x} denotes the average LUCE in BTH area; w_{ij} represents spatial weight matrix (this study used a neighboring

Table 1. Carbon emission coefficient of land use types.

| Land use types | Carbon emission coefficient(t/(hm ² ·a) | Reference sources |
|----------------|--|-------------------|
| Cropland | 0.4595 | [35, 36] |
| Forestland | -0.6125 | [37] |
| Grassland | -0.022 | [38] |
| Water bodies | -0.0253 | [21, 38] |
| Unused land | -0.0005 | [12, 21] |

Note: the positive and negative coefficients represent carbon sources and carbon sinks, respectively.

Table 2. The estimation coefficients of indirect carbon emissions at county-level.

| Cities | Regression coefficients | Intercept | R ² |
|---------|-------------------------|-----------|----------------|
| Beijing | 0.701** | -1.991 | 0.701 |
| Tianjin | 1.687** | -17.687 | 0.774 |
| Hebei | 4.366** | -29.335 | 0.881 |
| BTH | 3.855** | -17.26 | 0.854 |

Note: **represents the significance at the level of 5%

weight matrix with Moran's I values between -1 and 1). The results of Moran's I greater than 0, less than 0, and equal to 0 reflected that there were spatial positive auto-correlation, negative auto-correlation and no auto-correlation, respectively. Higher values of Moran's I indicate greater spatial aggregation of LUCE. G_i denotes the local Moran's I standardized by Z-score method.

The Local Indicators of Spatial Association (LISA) was according to the local Moran's I . The LISA spatial aggregation map of LUCE results was divided into four types: High-High (H-H) and Low-Low (L-L) reflected positive spatial autocorrelation, High-Low (H-L) and Low-High (L-H) reflected negative autocorrelation.

Random Forest Model

The random forest method is a machine learning algorithm based on a decision tree, which can evaluate the relationship between independent and dependent variables and calculate the relative importance of covariates [39]. The bootstrap resampling technique was used to randomly extract a subset of training samples from the original training sample, and then generated multiple decision trees according to the training sample, the results of regression model were determined by the voting scores of the decision trees [25]. In this study, we built 1 km × 1 km with 21007 grids at county-level, and took the value of LUCE of each county in BTH as the dependent variable, and social-economic factors as the independent variable. In addition, we calculated Mean Decrease Accuracy (%IncMSE) to measure the importance of independent variables in LUCE, a higher value of %IncMSE indicates higher importance of the variables. According to the previous study [32, 40], the parameters were set as follows: ntree = 3000, mtry = 4. The RF regression was performed by R language platform. To reduce the relative error of the computational results. We randomly divided the total sample data into training sample (60%) and validation sample (40%), and then repeated the complete data into 5 times to generate 5 random sub-samples. We selected the feature variables that occurred at least three times ($\alpha = 0.05$) from the five training samples to calculate the final complete sample.

Geographically Weighted Regression Model

(GWR) model is a local linear regression model considering the spatial heterogeneity of variables [34-36]. This study used GWR to explore the spatial differentiation of variables driven by LUCE change. The equation of GWR model is as follows:

$$y_i = \beta_0(u_i, v_i) + \sum_{k=1}^n \beta_j(u_i, v_i)x_{ij} + \varepsilon_i \quad (6)$$

Where y_i is dependent variable; β_0 is the intercept term; (u_i, v_i) represents the coordinates of sample point i ; $\beta_j(u_i, v_i)$ refers to the regression coefficient

j of the sample parameter i , which reflects the spatial differentiation of the influence of different parameters; i and k represents random error term and the number of independent variables, respectively. The GWR 4.0 software was used to construct the model and ArcGIS 10.5 was then calculated the spatial distribution map in BTH.

Results and Discussion

Spatial-Temporal Analysis of LUCE at County-Level

In terms of carbon source of counties (Fig. 3), construction land was the primary carbon source in BTH, and its total carbon emission increased from 3155.77×10^4 t in 1992 to 14183.03×10^4 t in 2018, accounting for 56.84% to 71.34% of the total carbon source, respectively. While the total carbon emissions of cropland showed a trend of increasing and then decreasing, which increased 1768.76×10^4 t in 1992-2000 and decreased 304.43×10^4 t in 2000-2018. With respect to carbon sink of counties, forestland was the main source of carbon sinks, increasing from 1280.5×10^4 t in 1992 to 3156.41×10^4 t in 2018, and the grassland also increased by 90.10×10^4 t during 1992-2018. This is mainly due to the rapid urbanization stage of BTH since 2000, and the rapid expansion of the farmland and water bodies in the counties were gradually occupied for construction land, resulting in the decline of carbon source function of the cropland [41].

While the carbon absorption of water bodies decreased from 2633.29×10^4 t in 1992 to 186.82×10^4 t in 2018. A possible explanation for this may be the effective results of implementation project of *returning* farmland to forest and Beijing-Tianjin sand source control in 1999, and the protection of state public welfare forest and returning farmland to forest in BTH [36], which led to most construction land converted into forestland and grassland. While the carbon uptake of unused land was relatively small, ranging from 0.39×10^4 t to 1.03×10^4 t, which was negligible in the study. From 1992 to 2018, the total net carbon emissions at county-level in BTH increased by 1300.04×10^4 t, with an average annual growth rate of 46.11% (Fig. 3a). Specifically, the average annual growth rate from 1992-2000, 2000-2010 and 2010-2018 were 41.33%, 39.51% and 38.06%, respectively (Fig. 3b).

Fig. 4 showed the significant differences of county LUCE in the BTH region. The spatial distribution of the county LUCE was characterized by high in the middle and low around. In this study, we used Jenks tool in ArcGIS 10.5 to classify the LUCE of each county in descending order: higher ($>154.43 \times 10^4$ t), high ($75.43-154.42 \times 10^4$ t), moderate ($35.26-75.42 \times 10^4$ t), low ($0.01-35.25 \times 10^4$ t) and lower ($<0 \times 10^4$ t). From 1992 to 2018. High-value counties of LUCE were mainly concentrated in BJ, TJ, TS eastern CZ and western HD, and gradually

expanded to the counties of QHD, southern CD and the central SJZ. The counties of LUCE above the moderate level showed an increasing trend, increasing from 75 counties (37.70%) in 1992 to 139 counties (69.84%) in 2018. While low-value counties of LUCE were scattered in XT, HS, northern CD and ZJK, demonstrating on a downward trend. The LUCE below the low-level

decreased from 126 counties (62.31%) in 1992 to 60 counties (30.15%) in 2018, which is primarily because of the different geographical locations, topographic features, and urbanization process of BTH counties [36]. For example, as the political and economic center of China, Beijing has introduced energy measures to control carbon consumption in counties [27],

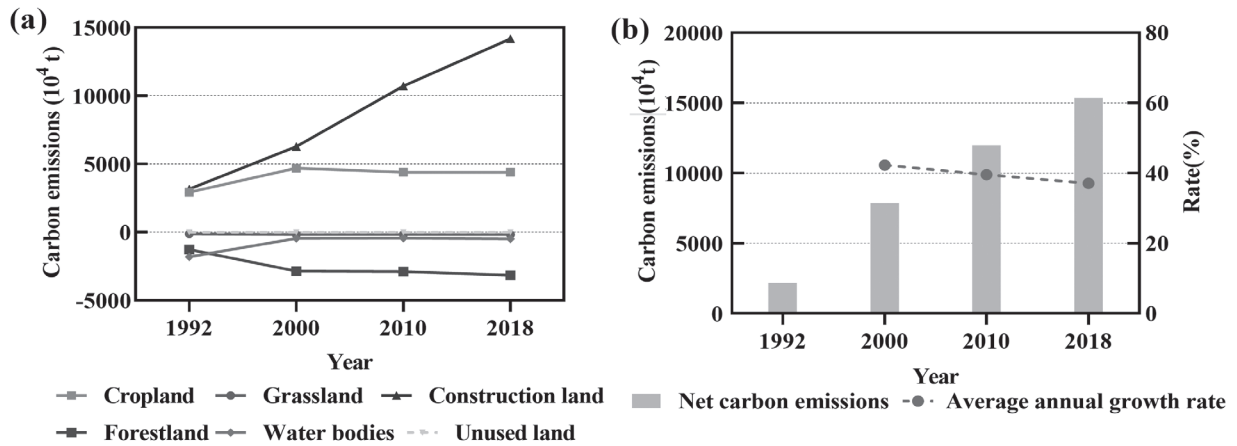


Fig. 3. a) Total carbon emission from different land use types and b) total net carbon emissions of counties from 1992 to 2018 in BTH.

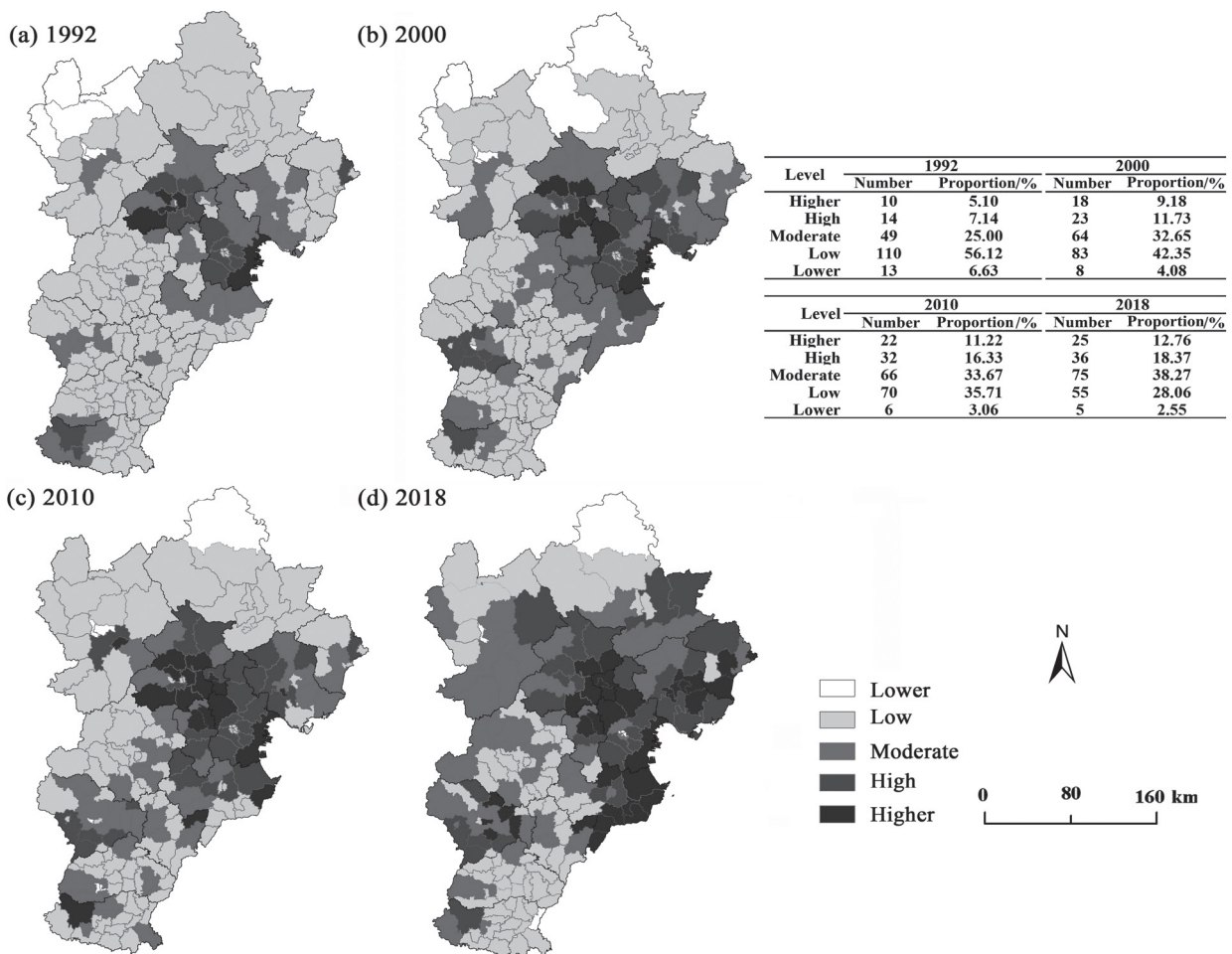


Fig. 4. Spatial distribution of the LUCE at county-level.

Table 3. Moran's *I* of county LUCE in BTH from 1992 to 2018.

| Year | Moran's <i>I</i> | Z-score | <i>p</i> -value |
|------|------------------|---------|-----------------|
| 1992 | 0.233 | 12.165 | 0.001 |
| 2000 | 0.272 | 10.019 | 0.001 |
| 2010 | 0.262 | 10.527 | 0.001 |
| 2018 | 0.323 | 9.341 | 0.001 |

but excessive human activities can increase the county's carbon emissions.

Analysis of Spatial Characterization of LUCE at County-Level

From 1992 to 2018, the global Moran's *I* for BTH counties ranged from 0.233 to 0.323 with a Z-score > 9.341 and a P-value < 0.001 (Table 3), indicating that the county-level LUCE in BTH was positively correlated and relatively spatially aggregated. From 1992 to 2018, the value of Moran's *I* raised 0.09, suggesting a gradual enhancement of spatial aggregation in the study area.

As shown in Fig. 5, from 1992 to 2018, the proportion of H-H counties increased by 2.55%, mainly concentrated in the counties of BJ, TJ and northern LF, and gradually expanded to the counties of QHD and southwest TS. While the proportion of L-L counties decreased by 7.65% from 1992-2010 and increased by 10.2% from 2010-2018, mainly distributed in HS, XT, HD, and western ZJK. Additionally, the H-H and L-L counties exhibited a clustering trend in the BTH region throughout the period. Moreover, L-H and H-L counties were randomly scattered around H-H and L-L regions, the L-H counties were mainly in Hedong district, Dongli district, and Hexi district of TJ and Mentougou district of BJ, with a slight decreased from 1992 to 2018. L-H areas were scattered in Xuanhua district of ZJK, Zhengding county, Jingjing county of SJZ, Yongnian district and Congtai district of XT. In conclusion, High-High and Low-High counties were distributed in the central core areas of BTH. While Low-Low and High-Low counties were clustered in the southern and northwestern suburbs of BTH. The results indicated that the counties of LUCE in BTH were vulnerable to the influence of their surrounding areas.

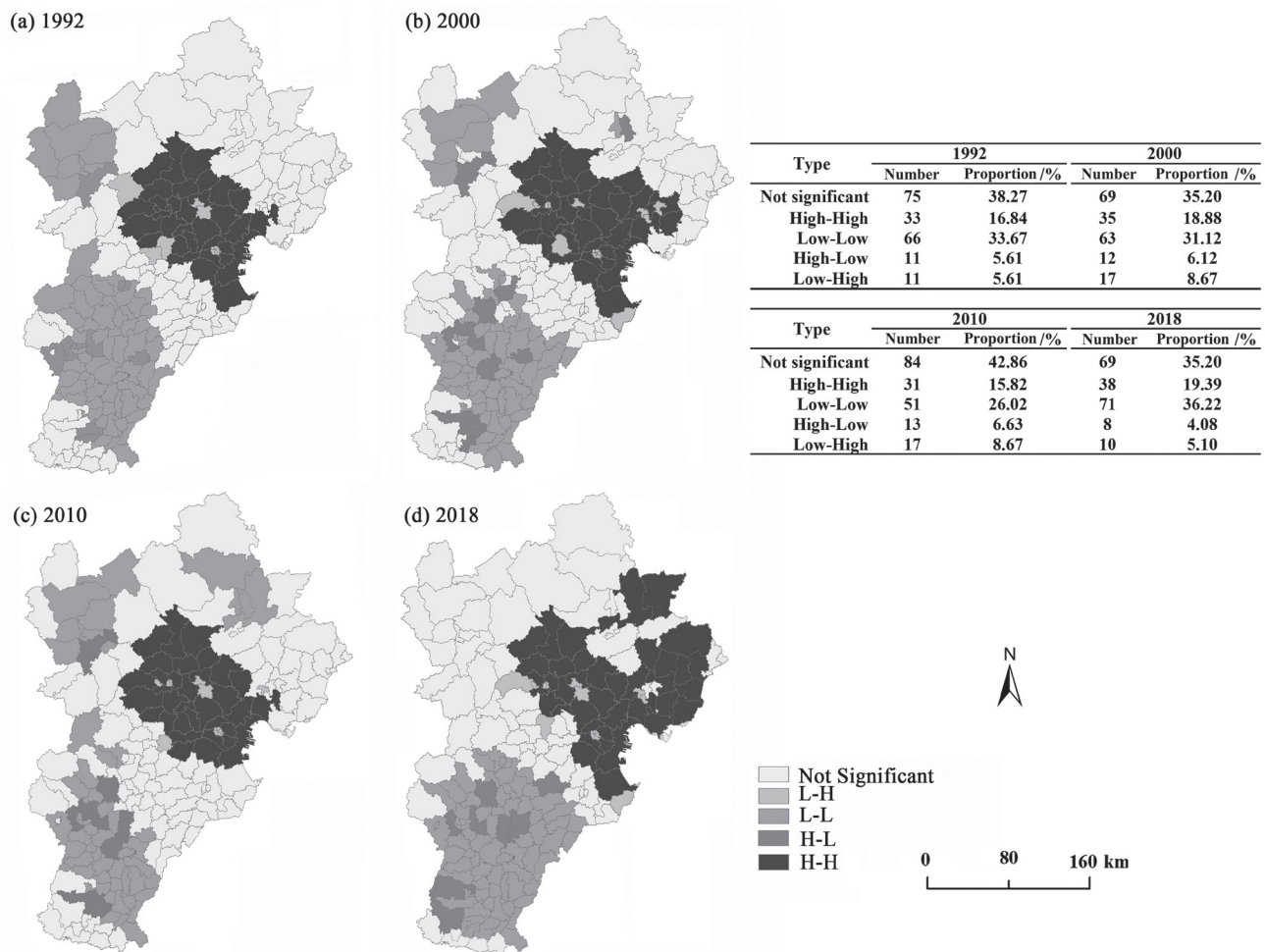


Fig. 5. LISA cluster map of LUCE from 1992 to 2018.

Table 4. The county LUCE verification by MLR and RF models.

| Model | R ² | RMSE | RSS | Correlation Obs vs. Pre |
|-------|----------------|------|-------|-------------------------|
| MLR | 0.56 | 3.22 | 15.36 | 0.764 |
| RF | 0.98 | 0.33 | 9.11 | 0.933 |

Note: R², RMSE and RSS represent the goodness of fit, mean square error, and residual sum of squares. The correlation obs vs. Pre denotes the correlation values between observed (obs) and predicted (pre) values

Analysis of Influencing Factors Based on Random Forest

Applicability of Random Forest Model

To further verify the applicability of RF model, in this study, we investigated and compared the fitting

results of multiple linear regression (MLR) and RF models [32]. As shown in Table 4, the R² and the correlation values between observed and predicted values of RF (0.98) were higher than that of MLR (0.56), while the RMSE and RSS of RF (0.33) model were lower than that of MLR (3.22).

Identification of Main Influencing Factors

The RF model was used to investigate the importance ranking of independent variables in sub-samples and complete sample from 1992-2018 (Fig. 6). Table 5 shows the significance of variables in each sample and complete sample. Of these factors, CGDP, SI, TI, PD, UR, ES, RND and TP were selected for the calculation of the final complete sample. As shown in the complete sample, PD was the most important factor affecting the county-level LUCE,

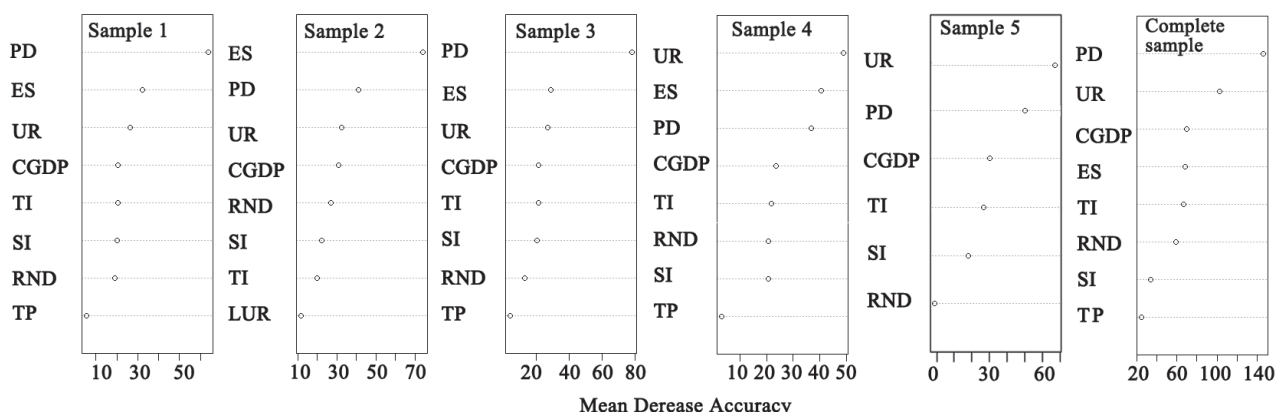


Fig. 6. Importance ranking of driving factors by random forest model.

Table 5. The significance of independent variables in each sample and complete sample.

| Variables | Sample 1 | Sample 2 | Sample 3 | Sample 4 | Sample 5 | Complete Sample |
|-----------|----------|----------|----------|----------|----------|-----------------|
| CGDP | Y | Y | Y | Y | Y | Y |
| LFE | N | N | N | N | N | N |
| PI | N | N | N | N | N | N |
| SI | Y | Y | Y | Y | Y | Y |
| TI | Y | Y | Y | Y | Y | Y |
| PD | Y | Y | Y | Y | Y | Y |
| UR | Y | Y | Y | Y | Y | Y |
| ES | Y | Y | Y | Y | N | Y |
| RND | Y | Y | Y | Y | N | Y |
| CLA | N | N | N | N | N | N |
| TP | Y | N | Y | Y | N | Y |
| LUR | N | N | N | N | N | N |

Note: Y and N indicate the variable is significant and non-significant, respectively

followed by US, CGDP, ES, TI, RND and SI, with TP and LUP having relatively less impact.

Spatial Heterogeneity of County LUCE Change Driven by Main Driving Factors

The regression coefficients of these factors in GWR model were shown in Table 6. There were significant differences between the maximum and minimum values of each factor coefficient, and their values varied widely. The regression coefficients of the main driving factors in GWR were then imported into ArcGIS for visual analysis (Fig. 7).

There was a significant positive correlation between PD and county LUCE, accounting for 78.58% of the total counties in the study area, and decreased from the center area to its surrounding counties. The counties of HD, XT, CZ and northwest ZJK showed a negative impact on the county LUCE (21.42%). The central BTH region, with high economic levels and favorable infrastructure will attract more people, The permanent resident population of 2018 in BTH of counties increased by 306.5 million people compared to 1992, which may lead to the expansion of construction land and transportation, further leading to more carbon emissions [18, 34].

Table 6. Regression coefficients in the GWR model.

| Variable | Minimum | Maximum | Mean | Std. | Positive value (%) | Negative value (%) |
|-----------|----------|---------|---------|---------|--------------------|--------------------|
| Intercept | -384.514 | 581.306 | 107.939 | 195.183 | | |
| PD | -0.011 | 0.034 | 0.021 | 0.004 | 78.58 | 21.42 |
| UR | -3.844 | 8.117 | 1.426 | 2.875 | 75.55 | 24.45 |
| CGDP | -0.001 | 0.008 | 0.002 | 0.001 | 60.72 | 39.28 |
| ES | -164.18 | 187.82 | 37.195 | 64.336 | 74.75 | 25.25 |
| TI | -5.514 | 1.766 | -1.400 | 1.725 | 68.84 | 31.16 |
| RND | -0.019 | 0.037 | 0.012 | 0.013 | 83.68 | 16.32 |
| SI | -2.82 | 0.84 | -0.841 | 0.942 | 37.24 | 62.76 |
| TP | -0.044 | 0.035 | -0.015 | 0.002 | 38.27 | 61.73 |

Note: Positive value represents the factors that have positive impact on LUCE of counties, the proportion represents the positive value counties in total counties of BTH; and negative values similarly

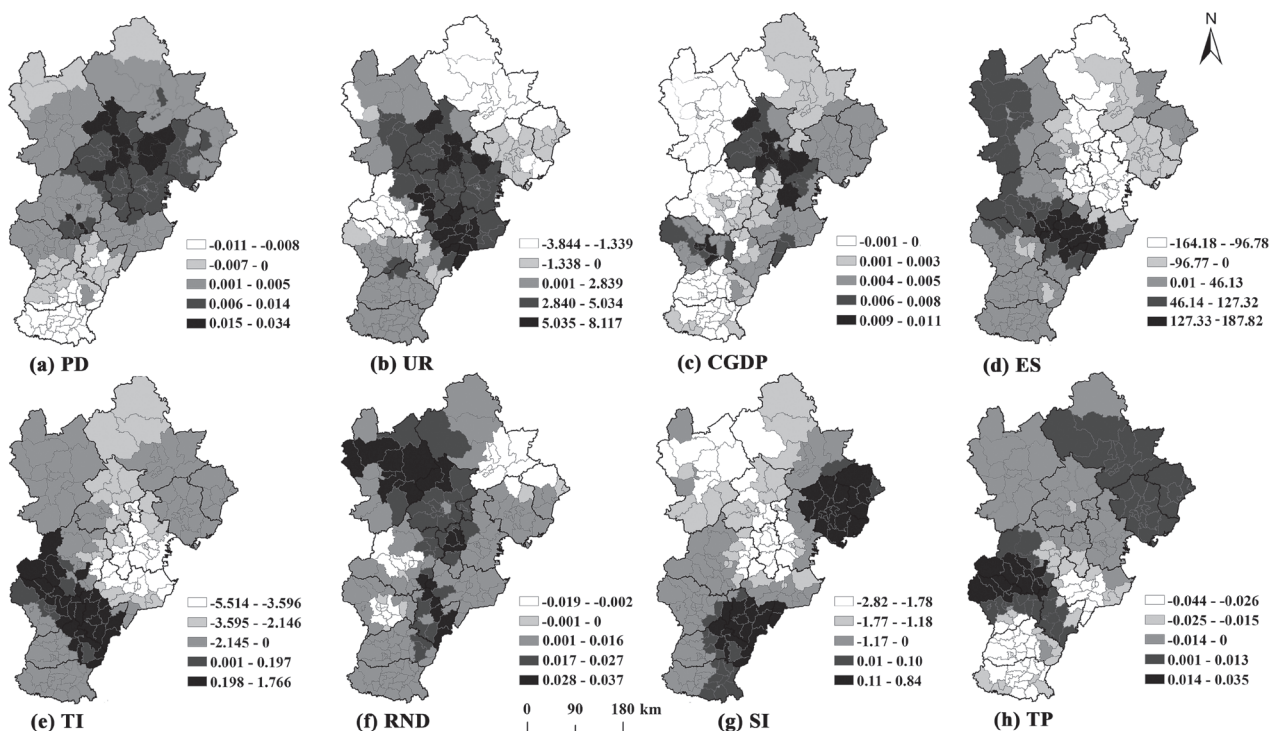


Fig. 7. Spatial distribution of regression coefficients between LUCE and its main driving factors.

The county regression coefficient of UR mainly had positive effects on 75.55% of county LUCE in BTH, and mainly in the central and southern counties of BTH, and presented negative coefficients (24.45%) scattered in the counties of CD, TS, QHD and southwest BD. CGDP brought positive coefficients in the central and eastern counties of BTH, and exerted a positive impact in 60.72% of total counties-the higher values were mostly in BJ, TJ and SJZ counties, and the negative coefficients (39.28%) in the western and southern BTH. The UR and CGDP factors, representing economic development, significantly increased the carbon emissions in BTH, which is in accord with earlier research [2, 10]. Some studies have pointed out that this is primarily because of the county siphon effects [42]: high LUCE values counties are highly urbanization and economy, which will attract superior resources and population from other counties. Although local governments have adopted a series of energy saving and emission reduction measures [37], with the improvement of living standards, citizens are pursuing a rich material life that these requirements brought about have increased carbon emissions. Thus, it is the responsibility of these counties to make more efforts to reduce carbon emissions in their economic development. While counties with negative coefficients indicate can be explained by the fact that local government had effectively controlled carbon emissions in these counties [43].

The positive coefficients between ES and county LUCE were 74.75% of total counties in BTH, and a negative effect in the remaining 25.25%. High carbon emission counties have more heavy industries and lower energy efficiency and technology, thus leading to higher levels of higher energy efficiency and technology energy consumption. On the other hand, the negative coefficient counties indicate that these counties are dominated by intensive production, advanced technology, and efficient management, which can effectively reduce county carbon emissions [36].

The effect of TI on LUCE of counties was mainly negative effects (68.84%), mostly in the northern and southwest counties of the study area, and the positive coefficient (31.16%) of CZ, northeast SJZ, HD and XT counties all showed great impact on the county LUCE. SI generated positive coefficients in the counties of QHD, TS, HS and eastern XT and SJZ (37.24%), and negative coefficients were primarily in the central and northwest counties (62.76%). The effect TI and SI on LUCE were mainly negative, which can be explained by many technology-intensive enterprises gathered in these counties, and the development of high-tech service industries may create an industrial agglomeration effect [44], which will promote production efficiency and technological innovation, thereby reducing energy consumption, while the counties of negative effect were in the initial stage of industry, and their industry structure lacks reasonable planning and layout, which generates more carbon emissions [45-46]. Moreover, we found the impact of the TI on county-level LUCE

was higher than that of the SI in the study area. Lin et al. [45] believed that with upgrading and optimizing industrial structure in China, the tertiary industry with low-carbon economy would gradually become the leading industry, and its impact on low-carbon emissions will exceed that of the secondary industry.

The coefficient of RND mainly presented positive coefficients (83.68%) in BJ, TJ, LF and ZJK, the negative coefficients scattered in the BD, CD and SJZ, accounting for 16.32% of the total counties in BTH, indicating that RND was also the major reason for the growth of LUCE, the increase RND will increase the county LUCE, which is in line with findings from earlier studies [5, 17]. In addition, the coefficients of TP presented a positive impact in 38.27% of total counties and a negative effect in the remaining 61.73%, with positive coefficients distributed in the counties of CD, QHD, TS and western BD and SJZ, and negative coefficients mainly in the north of BTH counties from southeast to northwest. The impact of the TP was both positive and negative in the study area, which is inconsistent with previous studies [2, 25]. In this study, we used the number of green patents to represent the TP. In fact, the development of green technologies is oriented to environmental needs and the results have complex lag characteristics. Thus, the coefficients of TP can be positive or negative. However, it is worth noting that although the growth rate of LUCE in BTH showed a gradually decreasing trend from 1992-2018, the continuous growth of LUCE in the study area cannot be ignored. This reveals the strict management of carbon emissions in BTH in the future, and more effort, measures and long-term strategies are required.

Conclusions

Land use carbon emissions data at county-level is difficult to obtain, while this study was solved by our study. The results revealed that the estimation method was feasible to investigate LUCE at county-scale. Above all, in order to summarize and illustrate the results visually, we used the nonlinear random forest model and GWR model to analyze the main drivers on the county LUCE and its spatial heterogeneity, the results showed RF had a better ability to explore the relationship between LUCE and its driving factors in the research area, again demonstrating that GWR model could visually reflect the social and environmental issues involving obvious spatial changes. Specifically, such results revealed which and where drivers might have influenced the county-level LUCE in BTH. These are the main finding of this study compared with previous research. The main conclusions are as follows:

(1) The BTH area was a carbon source with rising carbon emissions. The dynamic of county LUCE in BTH showed significant spatial-temporal heterogeneity, and its distribution presented an increasing trend from 1992 to 2018, with total net carbon emissions and

average annual growth rate increasing by 1300.04×10^4 and 46.11%, respectively. The spatial distribution of the county LUCE was characterized by high in the middle and low in the surroundings. The higher-value areas were primarily concentrated in the core areas of BTH counties and lower-value areas in the suburban counties within BTH.

(2) Obvious spatial agglomeration was also revealed, with the overall value of spatial autocorrelation increasing from 0.233 to 0.323 during 1992-2018, mainly showing High-High and Low-Low agglomeration types.

(3) Compared to MLR ($R^2 = 0.56$), the RF model had a better ability ($R^2 = 0.98$) in the estimation of LUCE dynamics caused by driving factors. RF method indicated population density had the greatest impact on county LUCE, followed by urbanization rate, per capita GDP, energy intensity, tertiary industry proportion, road network density, secondary industry proportion and technical progress, while the impact of primary industry proportion and land use policy was relatively small.

(4) The results of the GWR model demonstrated the eight main influencing factors were significant with positive and negative effects on county LUCE, the impacts of population, urbanization, economic, energy structure and road factors in the central core counties were significantly higher than in the northwestern and southern counties. Industrial structure and technology factors had the greatest impact in the southern and northeastern counties.

Appendix

Table A1. Carbon emission conversion coefficients of main energy sources.

| Energy type | Conversion coefficient of standard coal | Carbon emission coefficient |
|-------------|---|-----------------------------|
| Coal | $0.7143 \text{ t} \cdot \text{t}^{-1}$ | 0.7559 |
| Coke | $0.9714 \text{ t} \cdot \text{t}^{-1}$ | 0.8556 |
| Crude oil | $1.4286 \text{ t} \cdot \text{t}^{-1}$ | 0.5860 |
| Gasoline | $1.4286 \text{ t} \cdot \text{t}^{-1}$ | 0.6182 |
| Kerosene | $1.4714 \text{ t} \cdot \text{t}^{-1}$ | 0.5538 |
| Diesel | $1.4714 \text{ t} \cdot \text{t}^{-1}$ | 0.5743 |
| Fuel oil | $1.4574 \text{ t} \cdot \text{t}^{-1}$ | 0.5918 |
| Natural gas | $1.33 \times 10^{-3} \text{ t} \cdot \text{m}^{-3}$ | 0.4483 |
| Electricity | $0.3450 \text{ t} \cdot \text{t}^{-1}$ | 0.2720 |

Acknowledgments

This research is supported by the National Natural Science Foundation of China (No. 41877533).

Conflict of Interest

The authors declare no conflict of interest.

References

- ELSUNOUSI A.A.M., SEVIK H., CETIN M., OZEL H.B., OZEL H.U. Periodical and regional change of particulate matter and CO₂ concentration in Misurata. *Environmental Monitoring and Assessment*, **193**, 707, **2021**.
- CETIN M., SEVIK H. Change of air quality in kastamonu city in terms of particulate matter and CO₂ amount. *Oxidation Communications*, **39** (4), 3394, **2016**.
- YANG H.R., ZHENG H., LIU H.G., WU Q. NonLinear effects of environmental regulation on eco-efficiency under the constraint of land use carbon emissions: Evidence based on a bootstrapping approach and panel threshold model. *International Journal of Environmental Research and Public Health*, **16** (10), 1679, **2019**.
- ZHAO Y., CHEN R., ZANG P., LH A., SM A., SW C. Spatiotemporal patterns of global carbon intensities and their driving forces. *Science of the Total Environment*, **818**, 151690, **2022**.
- YUAN Y., CHUAI X.W., XIANG C.Z., GAOR. Carbon emissions from land use in Jiangsu, China, and analysis of the regional interactions. *Environmental Science And Pollution Research*, **1**, **2022**.
- XU R., SUN Z.Y. Analysis of influencing factors of land use carbon emission based on STIRAP model: A case study of Duolun county, Inner Mongolia. *International Journal of Environmental Research*, **2** (12), **2021**.
- LUN F., JOSEP G.C.L., XU Z.Q., HE L., ZHENG Y. Residential energy consumption and associated carbon emission in forest rural area in China: A case study in Weichang County. *Journal of Mountain Science*, **11**, 792, **2014**.
- WANG R., YOU L., ZHANG H. Carbon emission governance zones at the county level to promote sustainable development. *Land*, **10** (2), 197, **2021**.
- CETIN M., SEVIK H. Measuring the impact of selected plants on indoor CO₂ concentrations. *Polish Journal of Environmental Studies*, **25** (3), 973, **2016**.
- SHEN X.Z., HUANG L., ZHU J., GAO J.J. Relationship between land use carbon emission and economic growth based on GIS. *Arabian Journal of Geosciences*, **14** (6), **2021**.
- ZHOU S.Y., XI F.M., YIN Y., MA M.J., ZHANG W.F. Accounting and drivers of carbon emission from cultivated land utilization in Northeast China. *Chinese Journal of Applied Ecology*, **32** (11), 3865, **2021**.
- YU W.M., ZHANG T.T., SHEN D.J. Analysis on the evolution of carbon emission intensity pattern and influencing factors at county level in China based on Stochastic Forest model. *Journal of Environmental Science*, **42** (6), 2788, **2022**.
- LONG Z., PANG J.X., LI S.K., ZHAO J.Y., YANG T., CHEN X.P., ZHANG Z.L., SUN Y.Q., LANG L.X., WANG N.F., SHI H.Y., Wang B. Spatiotemporal variations and structural characteristics of carbon emissions at the county scale: a case study of Wu'an City. *Environmental Science And Pollution Research*, **2022**.
- ZHANG J., CHEN H., LIU D., SHI Q.Q., GENG T.W. The spatial and temporal variation and influencing factors of land use carbon emissions at county scale. *Journal of*

- Northwest University (Natural Science Edition), **52** (1), 21, **2022**.
15. LV Q., LIU H., WANG J., LIU H., SHANG Y. Multiscale analysis on spatiotemporal dynamics of energy consumption CO₂ emissions in China: Utilizing the integrated of DMSP-OLS and NPP-VIIRS nighttime light datasets. *Science of the Total Environment*, **703**, 134394, **2020**.
 16. LIU Y., YANG Y., JING W., YAO LING., YUE X.F., ZHAO X.D. A new urban index for expressing inner-city patterns based on MODIS LST and EVI regulated DMSP/OLS NTL. *Remote Sensing*, **9** (8), 777, **2017**.
 17. CHENG H., QZ B., XING M., HG D., JI H. An improved nighttime threshold method for revealing the spatiotemporal dynamics and driving forces of urban expansion in China. *Journal of Environmental Management*, **289**, 112574, **2021**.
 18. ZHANG C., ZHAO L., ZHANG H., CHEN M.N., FANG R.Y., YAO Y. Spatial-temporal characteristics of carbon emissions from land use change in Yellow River Delta region, China. *Ecological Indicators*, **136**, 108623, **2022**.
 19. CHEN J., CHENG S., SONG M. Changes in energy-related carbon dioxide emissions of the agricultural sector in China from 2005 to 2013. *Renewable & Sustainable Energy Reviews*, **94**, 748, **2018**.
 20. WANG Y. The spatial distribution characteristics of carbon emissions at county level in the harbin-changchun urban agglomeration. *Atmosphere*, **12**, **2021**.
 21. CETIN M., ONAC A.K., SEVIK H., SEN B. Temporal and regional change of some air pollution parameters in Bursa. *Air Quality Atmosphere and Health*, **12**, 311, **2019**.
 22. WU L., JIA X., GAO L., ZHOU Y.Q. Effects of population flow on regional carbon emissions: evidence from China. *Environmental Science and Pollution Research*, **28** (44), 62628, **2021**.
 23. CHUAI X., HUANG X., QI X., LI, J., ZUO T., LU Q., LI J. B., WU C.Y., ZHAO R.Q.A. preliminary study of the carbon emissions reduction effects of land use control. *Scientific Reports*, **6**, 36901, **2016**.
 24. RONG T., ZHANG P., JING W., ZHANG Y., LI Y., YANG D. Carbon dioxide emissions and their driving forces of land use change based on Economic Contributive Coefficient (ECC) and Ecological Support Coefficient (ESC) in the Lower Yellow River Region (1995-2018). *Energies*, **13** (10), 1, **2020**.
 25. ZHANG D., WANG Z., LI S., Li S. C., Zhang H. W. Impact of land urbanization on carbon emissions in urban agglomerations of the middle reaches of the Yangtze River. *International Journal of Environmental Research and Public Health*, **18** (4), 1403, **2021**.
 26. WANG Y., NIU Y., LI M., YU Q., CHEN, W. Spatial structure and carbon emission of urban agglomerations: Spatiotemporal characteristics and driving forces. *Sustainable Cities and Society*, **78**, 103600, **2021**.
 27. YANG S., JI Y., ZHANG D., FU J. Equilibrium between road traffic congestion and low-carbon economy: A case study from Beijing, China. *Sustainability*, **11** (1), **2019**.
 28. ZHAO R., HUANG X., LIU Y., ZHONG T.Y., DING M.L., CHUAI X. W. Carbon emission of regional land use and its decomposition analysis: A case study of Nanjing City, China. *Chinese Geographical Science*, **25** (2), 198, **2015**.
 29. CUI H., ZHAO T., SHI H. STIRPAT-based driving factor decomposition analysis of agricultural carbon emissions in Hebei, China. *Polish Journal of Environmental Studies*, **27** (4), 1449, **2018**.
 30. SUN Y., ZHAO T., XIA L. Spatial-temporal differentiation of carbon efficiency and coupling coordination degree of Chinese county territory and obstacles analysis. *Sustainable Cities and Society*, **76**, 103429, **2022**.
 31. XU Q., DONG Y X., YANG R. Urbanization impact on carbon emissions in the Pearl River Delta region: Kuznets curve relationships. *Journal of Cleaner Production*, **180**, 514, **2018**.
 32. TIAN C., CHENG L.L., YIN T. T. Impacts of anthropogenic and biophysical factors on ecological land using logistic regression and random forest: A case study in Mentougou District, Beijing, China. *Journal of Mountain Science*, **19** (2), 433, **2022**.
 33. WEN Y., WU R., ZHOU Z., ZHANG S.J., YANG S.G. A data-driven method of traffic emissions mapping with land use random forest models. *Applied Energy*, **305**, 117916, **2022**.
 34. ZHOU Q. L., WANG C. X., FANG S. J. Application of geographically weighted regression (GWR) in the analysis of the cause of haze pollution in China - ScienceDirect. *Atmospheric Pollution Research*, **10** (3), 835, **2019**.
 35. LI C., ZHANG L., GU Q. Spatio-Temporal differentiation characteristics and urbanization factors of urban household carbon emissions in China. *International Journal of Environmental Research and Public Health*, **19** (8), **2022**.
 36. HUANG X., LIU J. Regional economic efficiency and its influencing factors of Beijing-Tianjin-Hebei metropolitans in China based on a heterogeneity stochastic frontier model. *Chinese Geographical Science*, **30** (1), 30, **2020**.
 37. CHEN W., MA J. The government coordination mechanism research on the coordinated development of Beijing-Tianjin-Hebei manufacturing. *International Conference on MEIC* **8**, 992, **2015**.
 38. CAMPOS C.P., MUYLAERT M.S., ROSA L.P. Historical CO₂ emission and concentrations due to land use change of croplands and pastures by country. *Science of the Total Environment*, **346** (1-3), 149, **2005**.
 39. GUO F., SU Z., TIGABU M. Spatial Modelling of fire drivers in urban-forest ecosystems in China. *Forests*, **8** (6), 1, **2017**.
 40. SCORNET E. Random Forests and Kernel Methods. *Ieee Transactions on Information Theory*, **62** (3), 1485, **2016**.
 41. ZHOU Y., CHEN M., TANG Z., MEI Z. Urbanization, land use change, and carbon emissions: quantitative assessments for city-level carbon emissions in Beijing-Tianjin-Hebei Region. *Sustainable Cities and Society*, **66** (3), 102701, **2021**.
 42. REN Y., REN X., HU J. Driving factors of China? city-level carbon emissions from the perspective of spatial spillover effect. *Carbon Manag*, **10** (6), 551, **2019**.
 43. LONG Z., ZHANG Z., LIANG S., CHEN X., YANG T. Spatially explicit carbon emissions at the county scale. *Resources Conservation And Recycling*, **173** (2), 105706, **2021**.
 44. WANG J., YANG F., ZHANG X. Analysis of the influence mechanism of energy-related carbon emissions with a novel hybrid support vector machine algorithm in Hebei, China. *Polish Journal of Environmental Studies*, **28** (5), 3475, **2019**.
 45. LIN Q., ZHANG L., QIU B., ZHAO Y., WEI C. Spatiotemporal analysis of land use patterns on carbon emissions in China. *Land*, **10** (2), 1, **2021**.
 46. XIE H., YANG M., LI F. An Empirical Study on the correlation between educational input and upgrading of industrial structure under the background of Beijing-Tianjin-Hebei Coordinated Development. *Educational Sciences-Theory & Practice*, **18** (5), 2519, **2018**.

